

MODELLING TRANSIENT TWO-DIMENSIONAL NON-LINEAR TEMPERATURES IN
NUCLEAR FUEL USING THE FEAT CODE*

M. TAYAL , S.D. YU** , C. MANU, R. ABOUD, D. BOWSLAUGH, L. FLATT

Atomic Energy of Canada Ltd.
2251 Speakman Drive, Mississauga, Ontario, Canada L5K 1B2

**Department of Mechanical Engineering, Ryerson Polytechnic University
Toronto, Ontario, Canada M5B 2K3

ABSTRACT

A capability to model transient two-dimensional heat conduction has been added to the FEAT code, and is described in this paper. Results from the test cases show excellent agreement between FEAT calculations and corresponding analytical solutions. An illustrative example discusses the transient temperature in the pellet during a hypothetical loss-of-coolant accident in a CANDU[®] 9 reactor. Two-dimensional calculations are performed to account for the effects of end-flux peaking and heat transfer through the endcaps. The case studies have shown that the net effect is to increase the peak pellet temperature by about 176°C, compared to the one-dimensional situation of no end-flux peaking and no axial heat transfer through the endcap. Nevertheless, the peak pellet temperature of 2154°C is well below 2840°C, the melting point of UO₂.

INTRODUCTION

During some high-temperature transients such as a loss-of-coolant accident (LOCA), axial variations in flux in a fuel element (end-flux peaking) and axial heat conduction through the endcap result in transient two-dimensional axisymmetric heat transfer. To enable assessments of such processes, the capability of the finite-element code FEAT (Tayal 1989) has been extended to include modelling of transient temperatures. The current version of the FEAT code can model steady-state as well as transient non-linear temperatures in two-dimensional solids of arbitrary shapes.

* Presented at the fifth International Conference on CANDU Fuel, Canadian Nuclear Society, Toronto, Canada. 1997 September 21-25.

[®] CANDU is a registered trademark of Atomic Energy of Canada Limited (AECL).

FEAT solves the classical equation for conduction of heat in two dimensional solids. The code can model heat conduction, internal generation of heat, prescribed convection to a heat sink, prescribed temperatures at boundaries, prescribed heat fluxes on surfaces and temperature-dependence of material properties such as thermal conductivity. The code also contains pre-programmed packages for the thermal conductivity of UO_2 as a function of temperature, burnup, and porosity; and internal heat generation as a function of radius, enrichment and burnup. These features support the use of FEAT for applications involving nuclear fuel.

The finite-element method makes FEAT versatile, and enables it to accurately simulate complex geometries such as the conical profile of the endcap and the dished surface of the pellet. The gap elements provide a very efficient method of simulating heat transfer between adjacent solids. The steady-state version of FEAT was initially developed in 1980 and has been described previously (Tayal 1989). Since then, it has been extensively used in design analyses of CANDU fuel. Currently, it is our standard tool for detailed thermal assessments of fuel. The transient version was developed in 1990. The major focus of the present paper is to describe the transient capability of FEAT along with the associated verification and validation. An illustrative example dealing with transient temperature in CANDU fuel experiencing power pulse and end-flux peaking is also presented.

MATHEMATICAL MODEL

The Fourier equation of heat conduction in a two-dimensional, thermally isotropic solid may be written as (Hsu 1986)

$$\rho c \frac{\partial T(x, y, t)}{\partial t} = \frac{\partial}{\partial x} \left[k \frac{\partial T(x, y, t)}{\partial x} \right] + \frac{\partial}{\partial y} \left[k \frac{\partial T(x, y, t)}{\partial y} \right] + q(x, y, t) \quad (1)$$

in the Cartesian coordinates,

$$\rho c \frac{\partial T(r, z, t)}{\partial t} = \frac{\partial}{\partial r} \left[k \frac{\partial T(r, z, t)}{\partial r} \right] + \frac{k}{r} \frac{\partial T(r, z, t)}{\partial r} + \frac{\partial}{\partial z} \left[k \frac{\partial T(r, z, t)}{\partial z} \right] + q(r, z, t) \quad (2)$$

in the r-z coordinates, and

$$\rho c \frac{\partial T(r, \theta, t)}{\partial t} = \frac{\partial}{\partial r} \left[k \frac{\partial T(r, \theta, t)}{\partial r} \right] + \frac{k}{r} \frac{\partial T(r, \theta, t)}{\partial r} + \frac{k}{r^2} \frac{\partial}{\partial \theta} \left[k \frac{\partial T(r, \theta, t)}{\partial \theta} \right] + q(r, \theta, t) \quad (3)$$

in the $r-\theta$ coordinates. In the above equations, T is temperature; ρ is density; c is the specific heat; q is heat generation rate per unit volume; k is thermal conductivity; x, y are Cartesian coordinates for a two-dimensional plane solid; $r-\theta$ are polar coordinates for a two-dimensional plane solid; $r-z$ are cylindrical coordinates for a two-dimensional axisymmetric solid. All thermal quantities and material properties vary with spatial coordinates and time.

The boundary conditions may contain prescribed convection to a heat sink, prescribed temperatures at boundaries, prescribed heat fluxes on surfaces, and adiabatic surfaces. In the code, the transient solution starts with initial conditions for the following parameters: temperatures in the sheath and the pellets, heat transfer coefficient between the coolant and the sheath outer surface, heat transfer coefficient between the pellet and the sheath inner surface, heat generation rate, and thermal properties.

Because the thermal conductivity, density, and specific heat are non-linear functions of temperature, the governing partial differential equation for temperature is solved using the finite-element method in conjunction with an incremental numerical algorithm. To be consistent with the steady-state version of the FEAT code, triangular finite-elements are used to discretize a two-dimensional solid. This permits accurate representation of complex geometries.

Following the standard practice used in the finite-element analysis of heat conduction, energy balance equation for each finite-element may be established using Gurtin's functional form of the Rayleigh-Ritz variational principle, or Galerkin method (Hsu 1986). This yields the following equation:

$$[C_e]\{\dot{T}\} + [K_e]\{T\} = \{Q_e\} \quad (4)$$

where $[C_e]$ is the element heat capacitance matrix, $\{T\}$ is temperature, $\{\dot{T}\}$ is the rate of change of temperature, $[K_e]$ is the element thermal conductivity matrix, and $\{Q_e\}$ is the element thermal load matrix. Detailed derivations of the above equations are provided in standard text books; see for example Hsu, 1986. Global energy balance equations may be formed by summing the energy balance equations for all the individual finite-elements.

Three numeric algorithms, the Crank-Nicholson method (Hsu, 1986), the Galerkin method (Owen and Hinton, 1980) and the backward substitution method (Huebner and Thornton, 1982), were implemented in the FEAT code for integration of transient heat transfer with respect to time. Each scheme has its own specific strength regarding convergence and accuracy. With the three options available in the FEAT code, users can choose the numeric scheme most appropriate for the particular situation being analyzed.

CONVERGENCE

Tests were conducted to study the sensitivity of transient temperatures to the size of the time increment. Results of one such test for CANDU fuel, illustrated in Figure 1, are obtained using different time increments. Figure 2 shows that when the time step size is halved - from 0.1 s to 0.05 s - the maximum temperature changes by only 0.2 % (5°C). Hence this size of time step provides a converged solution for this and similar situations.

VERIFICATION AND VALIDATION

To validate the computer code, FEAT results were compared with three analytical solutions given by Chapman (1974), Kakac and Yener (1985) and results of the ELOCA⁺ code for one-dimensional transient temperatures (Sills 1979).

Heat conduction in a rectangular slab of 100 mm by 100 mm, receiving heat at a constant flux rate of 4 W/cm² from the side $x = 0$, is studied in test case 1. The initial temperature is 500°C everywhere in the slab. The material properties are $\rho = 10\,000\text{ kg/m}^3$, $c = 500\text{ J/kg}\cdot\text{°C}$. The initial thermal conductivity is 4.21 W/m•°C. The temperature dependence of the thermal conductivity is given by $k = 5.59 - 0.00276T\text{ W/m}\cdot\text{°C}$. Results given in Figure 3 show that the maximum difference between the FEAT and the analytical solution (Kakac and Yener 1985) for temperature at $x = 25\text{ mm}$ and $y = 0$ is within 0.4% (about 2°C).

Test case 2 involves a rectangular slab of side lengths of $a = 56\text{ mm}$ and $b = 11.2\text{ mm}$. Initially, the temperature is 300°C everywhere in the slab. At time $t = 0$, temperatures at sides $x = 0$ and $x = a$ are suddenly changed to 400°C. The material properties for the slab are $\rho = 6,490\text{ kg/m}^3$, $c = 350\text{ J/kg}\cdot\text{°C}$ and $k = 24\text{ W/m}\cdot\text{°C}$. In preparing the input for FEAT, a total of 102 finite-element nodes are used in the finite-element model. Comparison between the FEAT calculations and the analytical solution in the form of a series (Chapman 1974) is shown in Figure 4 for temperature at $x = 26.52\text{ mm}$ and $y = 0$. The maximum difference between the two solutions is 0.07% (about 0.2°C).

Heat conduction in a long solid cylinder of radius $r = 10\text{ mm}$ and length $L = 50\text{ mm}$ is studied in test case 3. The initial temperature in the cylinder is 300°C everywhere. At time $t = 0$, the cylinder is suddenly immersed in a heat sink of constant temperature 20°C. The material properties for the cylinder are $\rho = 10\,000\text{ kg/m}^3$, $c = 500\text{ J/kg}\cdot\text{°C}$ and $k = 40\text{ W/m}\cdot\text{°C}$. The heat transfer coefficient between the heat sink and the cylinder surface is 4,000 W/m²K. In this case, a total of 208 finite-element nodes are used in the finite-element model. Results of temperature

⁺ A one-dimensional finite difference code for transient temperature calculation.

at $r = 0$ and $z = 0$ shown in Figure 5 indicate that the maximum difference with analytical solution is within 3% (about 3°C).

In test case 4, the transient temperature in CANDU fuel experiencing power pulse but no end-flux peaking was calculated using the two-dimensional finite-element code, FEAT, and one-dimensional finite difference code, ELOCA. The main objective of this test case is to compare FEAT results with those of ELOCA for a one-dimensional heat transfer problem. Figure 6 shows, for a typical power pulse, the peak temperatures in the pellet, calculated using ELOCA and FEAT are very close for the period of power pulse. The maximum difference between the two codes is about 2% (38°C).

APPLICATIONS

The FEAT code was used to calculate the transient temperature in fuel pellets and sheath near the end caps during a LOCA in a CANDU 9 reactor. The main objective was to do a sensitivity analysis to establish the effect on the maximum fuel temperature and increase due to the end-flux peaking.

In a typical CANDU fuel temperature assessment, fuel centreline temperatures are predicted under the assumption that fuel power is axially uniform. In reality, the flux profile increases abruptly near the ends of fuel elements, due to the reduced amount of absorbing material. The flux peaking at the ends of a fuel element result in higher fuel pellet centerline temperatures at the ends than would be predicted by an axially symmetric simulation assuming uniform flux at the element average.

During the transient, rapid coolant voiding increases the power until, a few seconds later, the reactor is automatically shut down by one of the two shutdown systems. At the same time, reduced flow decreases the fuel/coolant heat transfer coefficient. End-flux peaking causes the heat generation rate to increase axially towards the end of the bundle, while axial heat conduction through the endcap provides extra cooling near the endcap.

Boundary conditions that must be considered to determine temperatures in the pellet, sheath and endcap, as shown in, Figure 1 are:

- No axial heat flow at $z = 60$ mm, an axial distance of approximately 3 pellet lengths beyond which the axial heat transfer is negligible.
- Convective boundary condition between the sheath outer surface and the coolant.
- Combined convective and radiative heat transfer between the pellet end surface and endcap inner surface.

- Heat transfer through conduction, radiation or convection between the pellet outer surface and the sheath inner surface.

Heat transfer coefficient from the pellet to the endcap depends mainly on the distance between the pellet and the endcap, their temperatures and the composition and temperature of the gas in the gap. These parameters all vary during the transient, and may vary spatially across the pellet-to-endcap interface. However, in the simulation, the heat transfer coefficient from the pellet to the endcap was assumed to be uniform and constant. The value chosen for this assessment was $1 \text{ kW/m}^2\cdot\text{K}$, which was found to give reasonable agreement between FEAT steady-state simulations and temperatures inferred from post-irradiation examinations of fuel bundles.

During the transient period, the power pulse data, end-flux peaking data, heat transfer data between the sheath and the coolant, heat transfer data between the sheath and pellet, and all other data are prepared using ELESTRES (Tayal 1987) and ELOCA (Klein et al, 1994) codes, and supplied to FEAT in the form of a data file. Material properties, e.g., density, heat capacity, thermal conductivity, are updated at the end of each time step using the correlations given in MATPRO-09 (1976) for UO_2 and Zircaloy.

A finite-element mesh consisting of 4,663 nodes, 8,316 elements, 211 convective boundary surfaces, and 196 gap elements was used. Time step of 0.1 s was used, based on a sensitivity study of convergence. For this discretization, it takes 5.3 min of central processor unit (CPU) time to complete the FEAT run on AECL's SGI computer.

Figure 7 shows typical profiles of pellet temperature along the fuel element centreline. Figure 7a shows the effect of end-flux peaking when it is assumed that neighbouring bundles remain in contact after the accident, whereas Figure 7b shows the results when it is assumed that neighbouring bundles separate after the accident. The latter case leads to higher flux peaking factors, and therefore higher temperatures.

End-flux peaking tends to increase pellet temperature near the endcap. On the other hand, extra conduction via the endcap tends to decrease pellet temperature in that region. The net result is that the maximum pellet temperature occurs at an axial distance of 12 to 15 mm from the outside of the endplate. The effects of axial heat transfer and end-flux peaking diminish as the distance from the endplate increases.

Figure 8 shows how the fuel centreline temperatures at $z = 14.7 \text{ mm}$ and $z = 57.9 \text{ mm}$ vary with time. The timing of the peak temperature is consistent with the power pulse profile. The peak temperature calculated using FEAT considering both end-flux peaking and axial heat transfer via endcap is about 176°C higher than that calculated using ELOCA. Nevertheless, the peak temperature occurs at the centreline and is predicted to be at about 2154°C , which is well below 2840°C , the melting point of UO_2 .

CONCLUSIONS

A capability for transient conduction of heat has now been added to the FEAT code. Test cases show that the calculations of FEAT agree well with independent analytical solutions. Assessment of pellet temperature during a Loss of Coolant Accident in the CANDU 9 reactor show that the combined influences of end-flux peaking and endcap cooling increase the pellet temperature by about 176°C compared to the situation without end-flux peaking and endcap cooling. The peak temperature in the pellet occurs at the centreline and is predicted to be at about 2154°C, which is well below the UO₂ melting point (2840°C).

ACKNOWLEDGEMENTS

The authors gratefully acknowledge the contributions of Z. Xu for providing independent analytical solutions and spreadsheet calculations for test case 1 and for reviewing this manuscript. Thanks are also due to D. Rattan for his review, and to J.H.K. Lau for encouragement, support, and review.

REFERENCES

- A.J. Chapman 1974 *Heat Transfer*, MacMillan, 3rd Ed, New York.
- T.-R. Hsu 1986 *The Finite Element Methods in Thermomechanics*, Allen & Unwin, Boston, MA.
- K.H. Huebner, E.A. Thornton 1982 *The Finite Element Method for Engineers*, John Wiley & Sons, New York.
- S. Kakac and Y. Yener 1985 *Heat Conduction*, Hemisphere Publishing Corporation, 2nd Ed., New York, NY.
- M.E. Klein, L.N. Carlucci and V.I. Arimescu 1994 "Simulation of In-reactor Experiments with the ELOCA.Mk5 Code", AECL-11133.
- MATPRO-9 - Version 09 1976 A Handbook of Materials Properties for use in the Analysis of Light Water Reactor Fuel Rod Behavior, TREE-NUREG-1005.
- D.R.J. Owen and E. Hinton 1980 *Finite Elements in Plasticity: Theory and Practice*, Pineridge Press Limited, Swansea, U.K.

M. Tayal 1987 "Modelling CANDU Fuel under Normal Operating Conditions: ELESTRES Code Description", AECL Report AECL-9331.

M. Tayal 1989 "The Finite Element Code FEAT to Calculate Temperatures in Solids of Arbitrary Shapes," *Nuclear Engineering and Design* 114, 99-114.

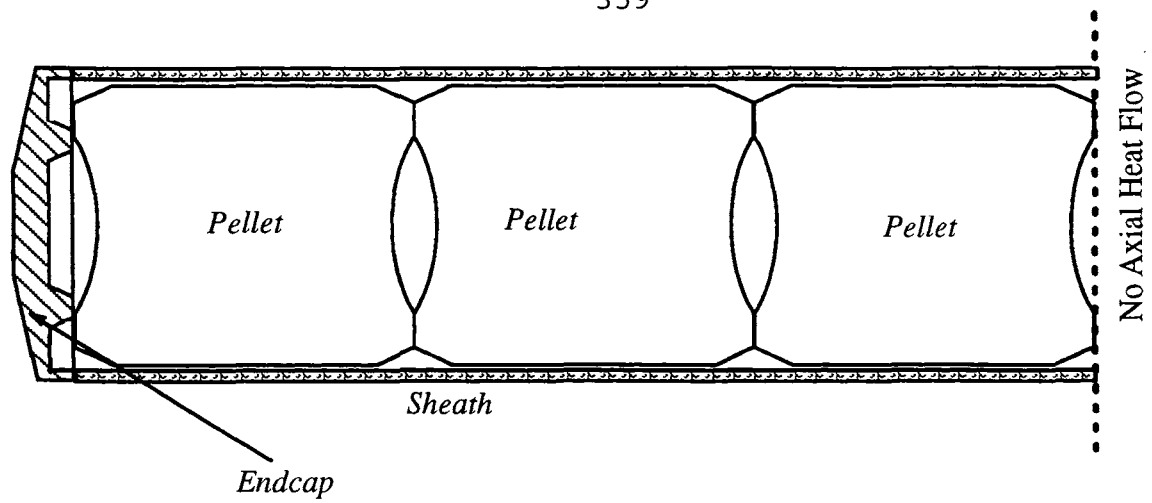


Figure 1 Schematic View of a Nuclear Fuel Element

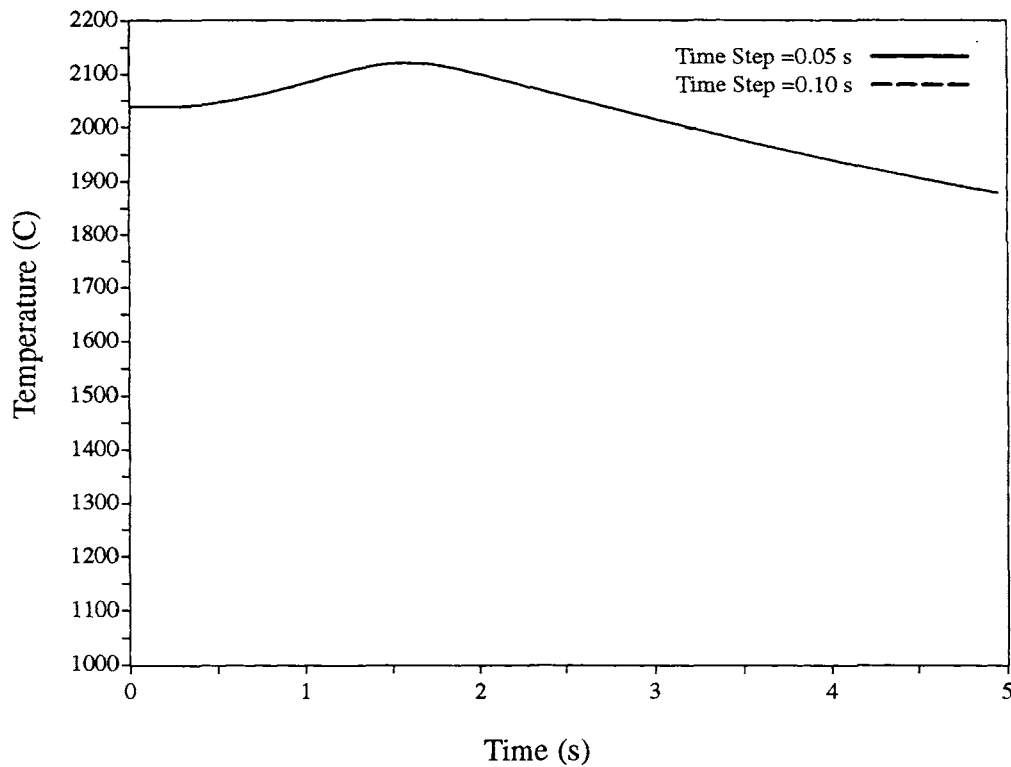


Figure 2 Convergence Test Results for Maximum Transient Pellet Centreline Temperature

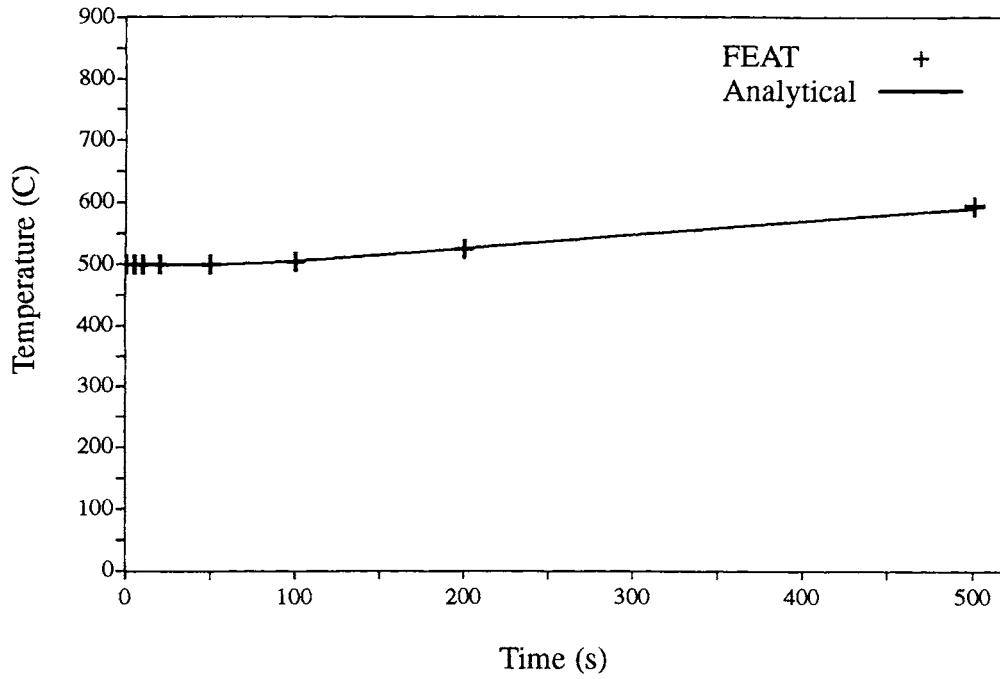


Figure 3 Transient Temperature at $x=25$ mm and $y=0$ for Test Case 1

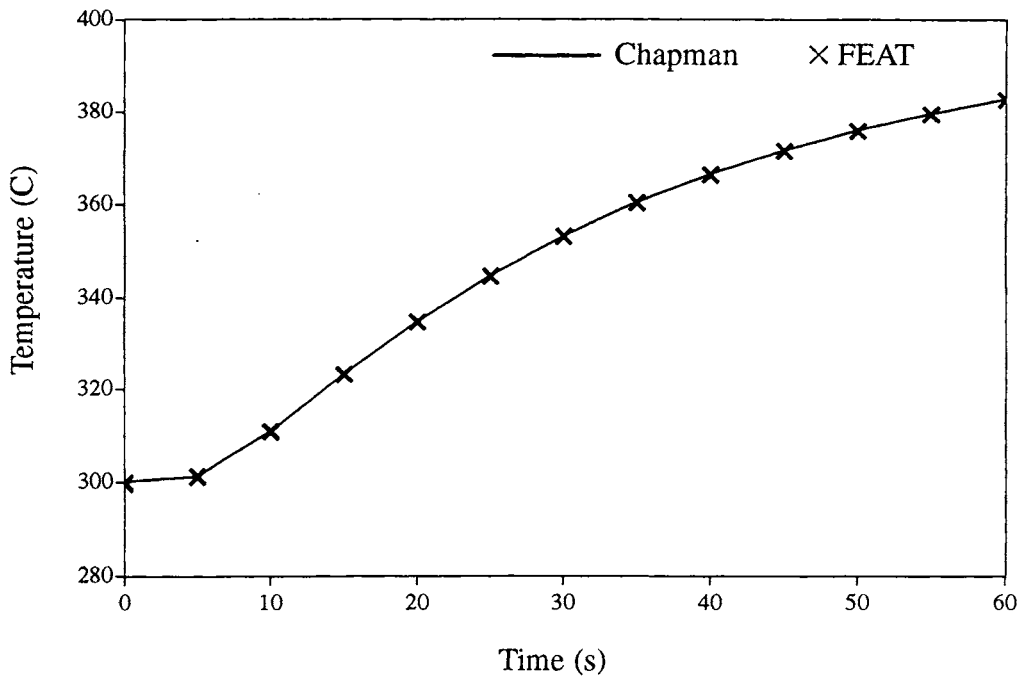


Figure 4 Transient Temperature at $x=26.52$ mm and $y=0$ for Test Case 2

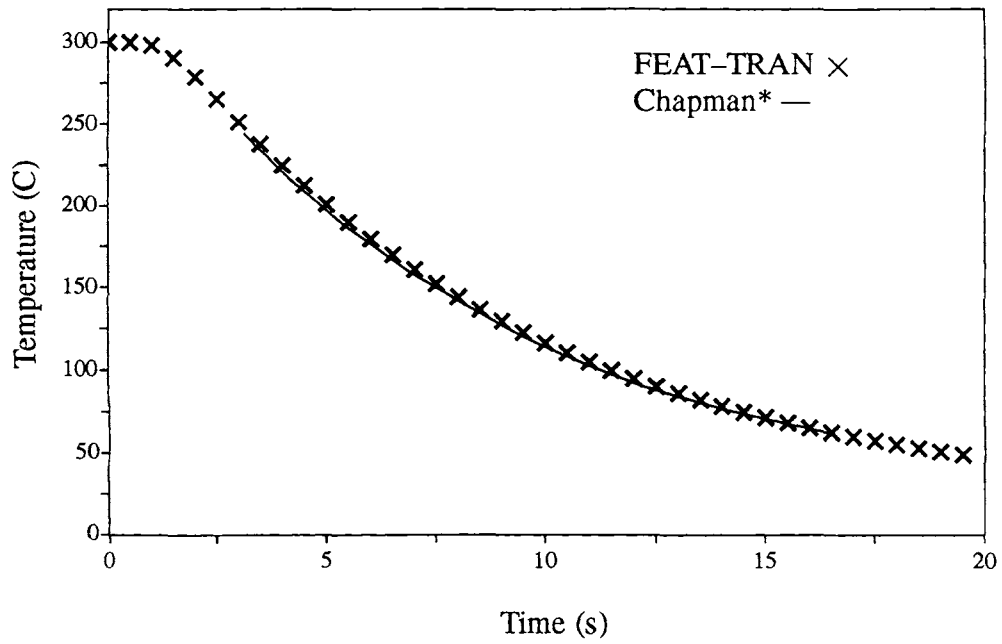


Figure 5 Transient Temperature at $r=0$ and $z=0$ for Test Case 3

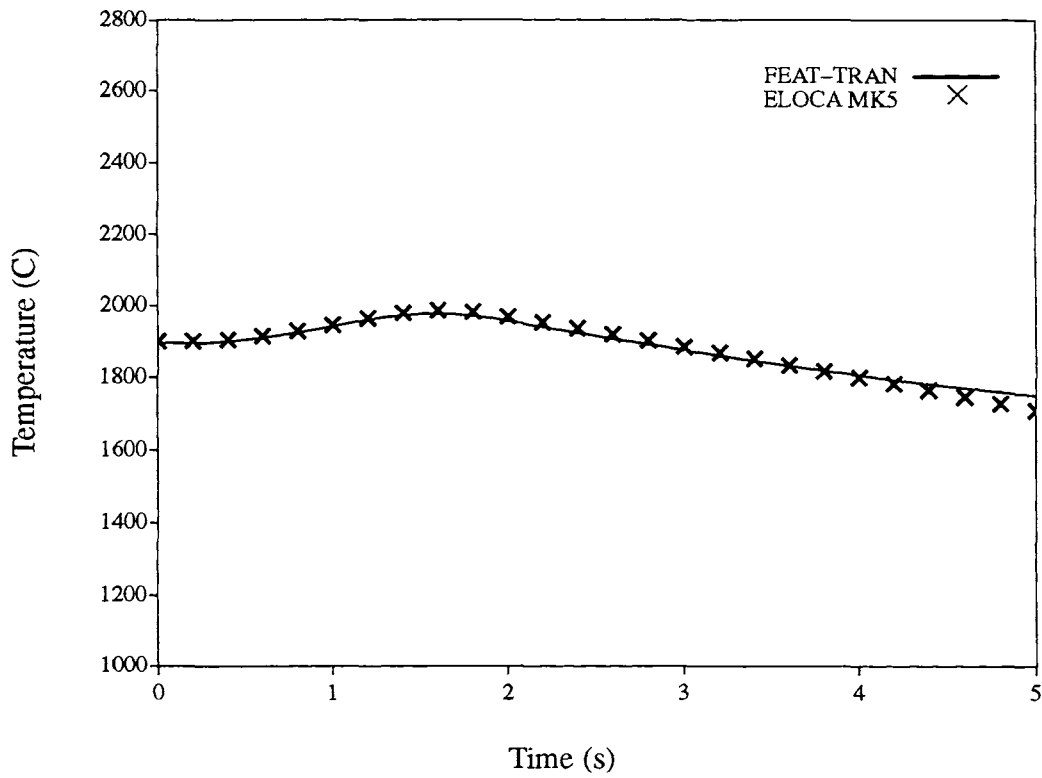


Figure 6 Transient Temperature at $r=0$ and $z=57.91$ for Test Case 4

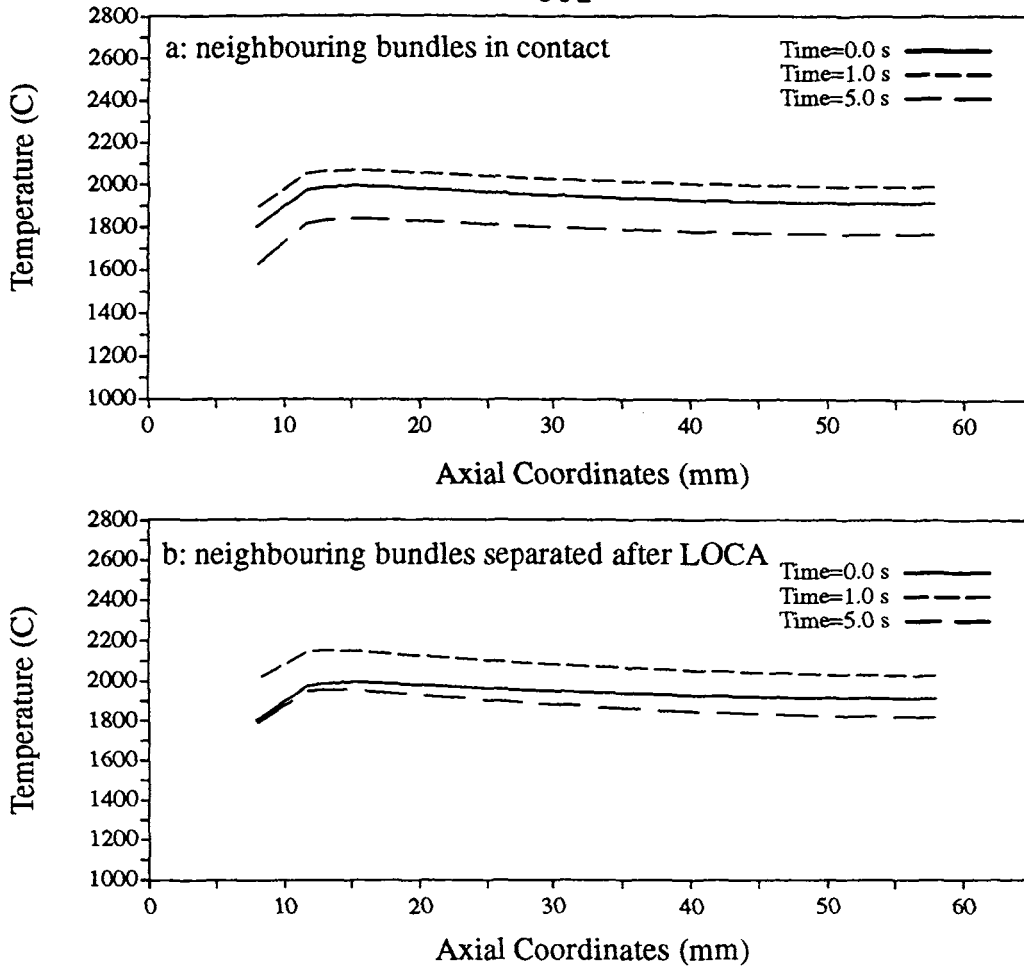


Figure 7 Transient Centreline Temperatures at Different Times for Two End-flux Peaking Profiles

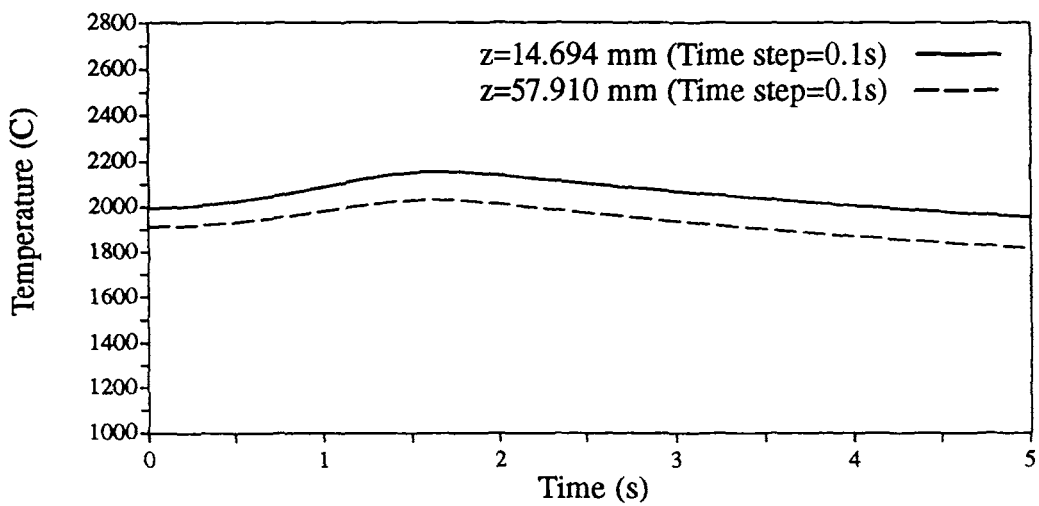


Figure 8 Transient Pellet Centreline Temperatures at Two Axial Locations vs. Time